

Phase-locking of 19-core Yb^{3+} – doped optical fibre

M. KOCHANOWICZ¹, D. DOROSZ^{1*}, and A. ZAJĄC^{1,2}

¹ Faculty of Electrical Engineering, Białystok University of Technology, 45d Wiejska St., 15-351 Białystok, Poland

² Institute of Optoelectronics, Military University of Technology, 2 Kaliskiego St., 00-908 Warszawa, Poland

Abstract. The supermode generation in a multicore optical fibre laser can be realised by phase-locking of radiation inside of the fibre. The model proposed by authors implies the achievement of supermode generation by exchanging radiation between the cores during the development of the laser action. The analysis of the impact of coupling value between the cores on phase radiation of particular emitters was considered. In the paper the phase-locking of 19-core optical fibre doped with Yb^{3+} ions is presented. The analysis of material and geometrical parameters of the active 19-core optical fibre and phase deviation on the beam quality factor of the laser beam in the far-field diffraction region has been analysed. The beam quality factor of the manufactured multicore fibre equals $\text{BQF} = 0.71$, $V = 2.4$, $d = 18 \mu\text{m}$. As a result of the conducted analysis a double-clad 19-cores optical fibre doped with ytterbium ions has been designed and fabricated and its luminescence spectra and far-field diffraction pattern have been measured. Registered in the experiment in MOFPA system far-field pattern showed centrally located peak of relatively high radiation intensity together with smaller side-lobes, and as such was similar to the pattern which had been obtained numerically.

Key words: multicore optical fibre, fibre lasers, ytterbium ions.

1. Introduction

Introduced in recent years double-clad multicore optical fibres offer new possibilities in the area of high-power short-length fibre lasers design [1–6]. In these fibres, the number of doping rare earth element ions is greater than in typical single-core fibres, proportionally to the number of cores. Moreover, placing multiple cores in fibre cladding makes it possible to reduce the length of the fibre which is necessary to absorb the pumping radiation [7–13]. If the radiation generated in individual cores is coherent, then in the far-field diffraction pattern a centrally located peak of high intensity and low divergence (i.e. supermode) is obtained, along with symmetrically placed side-lobes of significantly lower intensity [14–18]. Angular divergence of the central peak decreases proportionally to the number of emitters (i.e. elements of the matrix) generating mutually coherent radiation (with the ratio $N^{0.5}$, N being the number of emitters). Furthermore, the width of a laser beam profile in a phase-locked multicore fibre is several times smaller than usual, which is impossible to achieve in a standard single-core active fibre [18–20]. Multicore fibres whose cores are placed in a common cladding make it possible to achieve higher power output in comparison to common double-clad fibres, but at the same time they safeguard good quality of laser beam. Besides, these fibres are marked by higher pump absorption, and allow for uniform excitation of all cores. Proper design of a multicore optic fibre should enable phase-locking of the radiation generated in each of the cores in the fibre working as a fibre laser.

2. Impact of the construction parameters of an active multicore fibre on the quality of emitted beam

Beam Quality Factor (BQF) is a parameter used for describing the quality of laser beam produced by a matrix of emitters generating in-phase radiation. It is defined as the ratio of optical power contained in the central peak to the total optical power of the beam in the near field [20, 21]. Hence, the parameter is dependent solely on the filling factor of the matrix of emitters ($t = (d - 2r)/2r$, where d – distance between cores, $2r$ – core diameter), and not on the number of the cores. It assumes lower values in the cases when emitters are located close to one another.

The presented article scrutinizes the influence of parameters related to construction materials and geometry of active multicore fibres on the values of BQF. As well as that, the impact of phase deviations which may occur under various circumstances on BQF in the far-field region is analyzed. The phase difference for radiation generated in the cores of a multicore fibre working a fibre laser is described by the standard deviation:

$$SD = \sqrt{\frac{1}{N} \sum_{i=1}^N (\Theta_i - \bar{\Theta})^2}, \quad (1)$$

where Θ_i – radiation phase in the i -th core, $\bar{\Theta} = (1/N) \sum_{i=1}^N \Theta_i$ average phase of the radiation generated in all cores, N – number of cores.

*e-mail: d.dorosz@pb.edu.pl

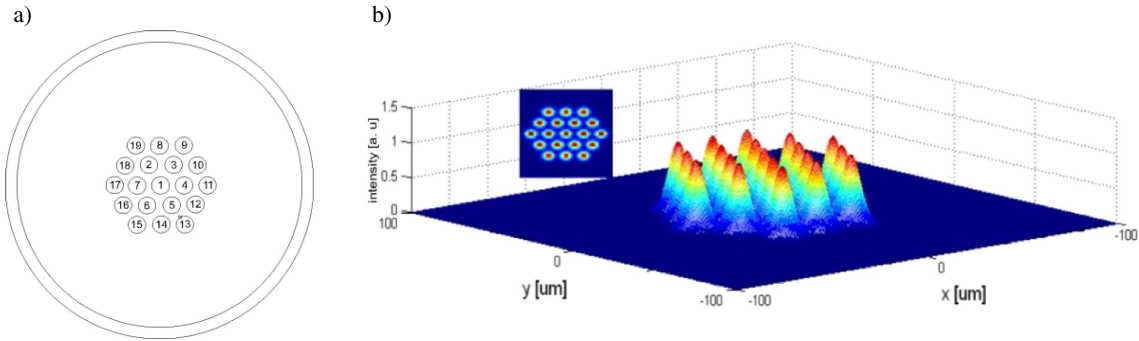


Fig. 1. Arrangement of cores (a), simulation of near field pattern (b) in the 19-core fibre

In the design of the 19-core fibre considered here, single-mode cores are located in the common inner cladding. An arrangement of cores and near – field of optical fibre are shown in Fig. 1. The diameter of the cores $2r = 10 \mu\text{m}$, the normalized frequency $V = (1.7 - 2.4)$, and the distance between core centres $d = (18 - 25) \mu\text{m}$. The spatial distribution of laser radiation emitted by individual cores is described by a Gaussian function.

$$E_m(x, y, z = 0) = A_m \exp \left[\frac{r^2}{w_0^2} + i\varphi_m \right], \quad (2)$$

where A_m – maximum amplitude in the m -th core, $r^2 = (x - mx_d)^2 + (y - ny_d)^2$, coordinates of the point, w_0^2 – mode area radius, φ_m – phase of radiation generated in the m -th core.

If the cores are considered as independent sources, then the field amplitude distribution of in the optic fibre can be described by the following formula:

$$E(x, y, z) = \sum_m A_m(z) E_m(x, y) e^{i\beta_m z}, \quad (3)$$

where A_m – field amplitude in the m -th core, β_m – propagation constant in the m -th core, E_m – field distribution in the m -th core.

Distribution of the electromagnetic field of the laser beam generated in the n -th core in the flat plane is described by the equation:

$$E_n(x, y, z) = \frac{w_0}{w(z)} \exp \left(- \frac{((x - x_n)^2 + (y - y_n)^2)}{w^2(z)} \right) \cdot \exp \left(-i \left\{ k \left[\frac{((x - x_n)^2 + (y - y_n)^2)}{2R(z)} + z \right] - \Psi + \Psi_{n0} \right\} \right), \quad (4)$$

where λ – radiation wavelength, (x_n, y_n) – coordinates of the central core, Ψ_{n0} – initial phase of the radiation in the n -th core,

$$k = \frac{2\pi}{\lambda}, \quad Z_0 = \frac{\pi w_0^2}{\lambda},$$

$$w(z) = w_0 \sqrt{1 + (z/Z_0)^2}, \quad R(z) = Z_0 \left(\frac{z}{Z_0} + \frac{Z_0}{z} \right),$$

$$\Psi = \arctan(z/Z_0).$$

Assuming that coupling occurs only between neighbouring cores, field distribution E_m in each of the cores is the sum of power generated in the core and the power received in effect of interference from adjacent cores:

$$\frac{dE_m}{dz} = -i\beta_m A_m(z) e^{-i\beta_m z} + \sum_n C_{m,n} A_n(z) e^{-i\beta_n z}, \quad (5)$$

where C – coupling coefficient.

The far-field diffraction pattern (in the Fraunhofer diffraction region) is described by the formula:

$$U(x, y, z_d) = \frac{e^{-ikz_d}}{i\lambda z_d} \cdot \iint U(x_1, y_1, z_1) e^{\frac{-ik}{z_d} [(x-x_d)^2 + (y-y_d)^2]} dx_1 dy_1, \quad (6)$$

where $k = \frac{2\pi}{\lambda}$, λ – wavelength, x_1, y_1 – coordinates of the cores, z_d – the length of observation.

Distribution of radiation intensity (i.e. the pattern) in the far-field is proportional to the time-averaged square of field amplitude $|U(x, y, z)|^2$ [22]. In order to establish the far-field pattern, a method employing two-dimensional fast Fourier transform (FFT) can be used [23]. Results of numerical simulations of the far-field patterns are presented below.

In the case when there is no interference between radiation emitted by individual cores in the fibre, each of the cores generates radiation separately (Fig. 2). Phases of the radiation emitted by the cores are random, and the radiation output power is the sum of powers emitted from all the cores singularly. In the considered situation, however, the intensity of the beam generated in the far-field is relatively low. The simulations of far-field pattern for the 19-core fibre generating mutually coherent radiation is shown in the following figures (Figs. 3–5).

The intensity of the central peak is significantly higher than in the case of emitters which work independently. With the increasing distance between cores the amount of energy in the side-lobes of the far-field pattern grows, which results in decrease of BQF (Figs. 5, 6a).

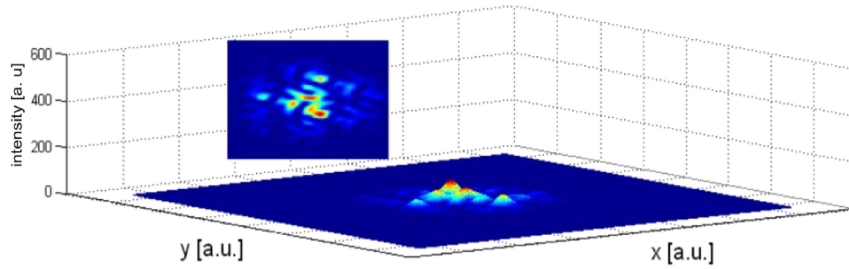


Fig. 2. Simulation of far-field diffraction pattern of 19 – core optical fibre – random phases, $2r = 10 \mu\text{m}$, $d = 18 \mu\text{m}$

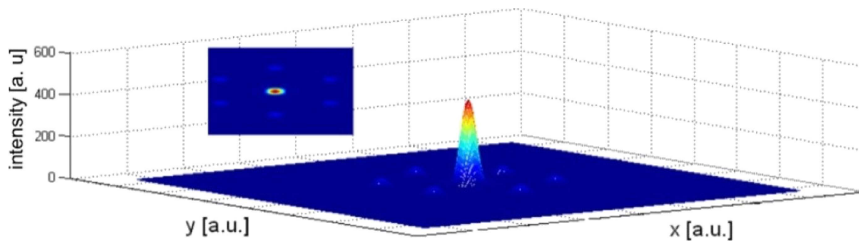


Fig. 3. Simulation of far-field diffraction pattern of 19 – core optical fibre – phase – locked (equal phases), $V = 2.4$, $d = 18 \mu\text{m}$

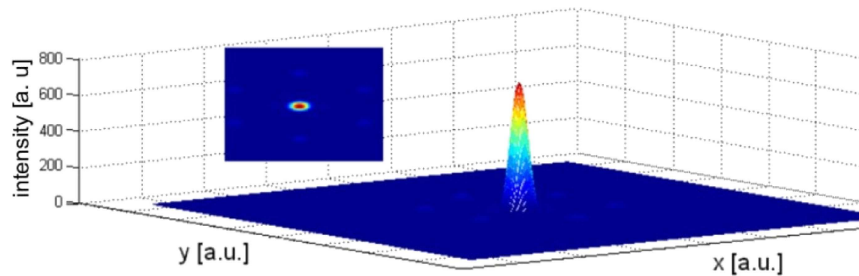


Fig. 4. Simulation of far-field diffraction pattern of 19 – core optical fibre – phase – locked (equal phases), $V = 2$, $d = 18 \mu\text{m}$

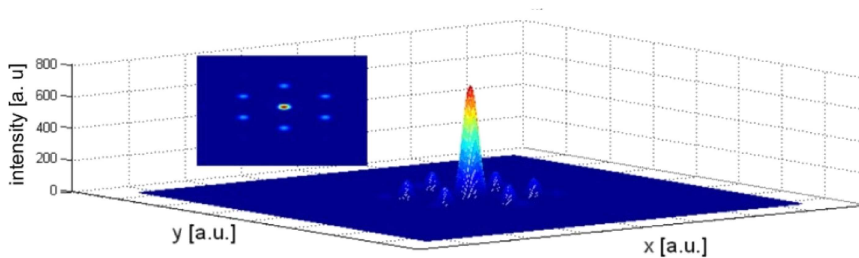


Fig. 5. Simulation of far-field diffraction pattern of 19 – core optical fibre – phase – locked (equal phases), $V = 2$, $d = 25 \mu\text{m}$

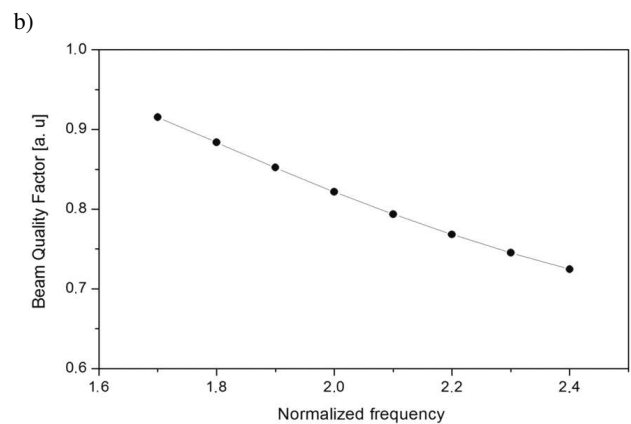
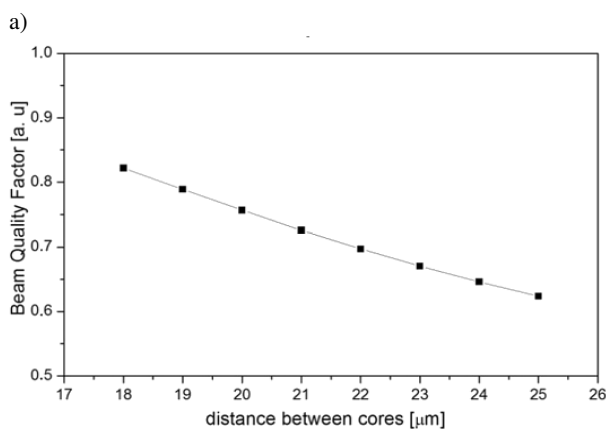


Fig. 6. Relation between BQF and: distance between cores (a), normalized frequency value (b) in the 19-core fibre

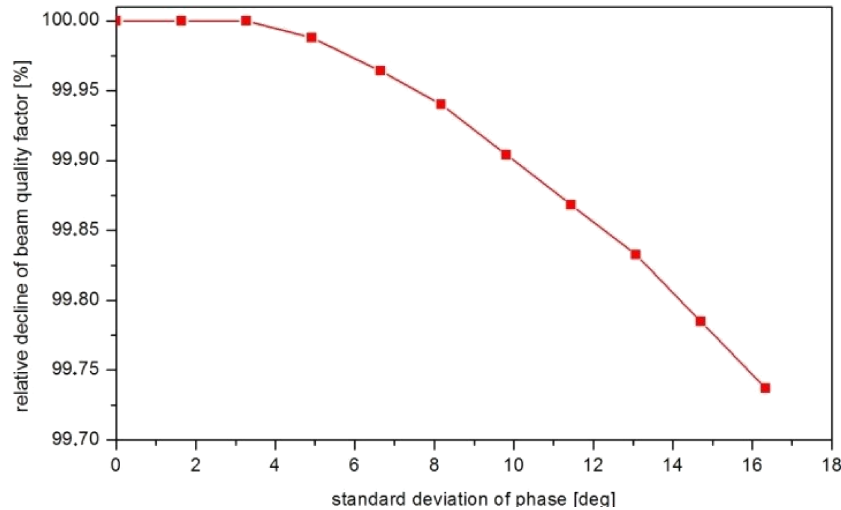


Fig. 7. Relative decrease of BQF as a function of standard deviation of radiation phase in the 19-core fibre

Improvement of BQF can be also achieved by lowering the normalized frequency value. In such conditions the ratio of central peak intensity to the energy contained in side-lobes is the highest (Fig. 6b). Figure 7 illustrates the impact of incomplete phase lock of the radiation generated in individual cores on the BQF in the far-field.

Investigation of the possible phase deviations in the cores indicates that the standard deviation below 14° remains practically without any influence on the far-field pattern for the fibre designs which are analyzed here. Relative decrease of BQF in the considered cases is below 0.3%.

3. 19-Core active optical fibre in a fibre laser system

Generating radiation in a fibre laser requires establishing time dependencies for qualities describing energy of electromagnetic field radiation (e.g. photon flux circulating in the resonator) as well as energy accumulated in active medium (e.g. optical gain, population inversion) [4]. In the conducted analysis concerning influence of partial radiation exchange between the fibre cores on the radiation phase differences between individual emitters during the development of laser action in a multicore fibre laser, an iterative method of following the photon flux was employed. In the interaction between laser impulse with the medium, the process of pumping is not visible, and only absorption of energy from the medium occurs. This phenomenon is related to the fact that the time in which the initial hundred passes of photons through the resonator takes place is significantly shorter in comparison to the upper laser level lifetime ($t_{imp} \ll \tau, W_P^{-1}$). It was assumed, then, that the medium would not be additionally pumped. Moreover, the model presupposes the existence of two photon fluxes in the resonator: J^+ and J^- which propagate in opposite directions. The fluxes are described by time and spatial functions, and they interact with each other through the boundary conditions

and active medium (amplifier). In the model of internal phase locking discussed in the present paper, the analyzed photon fluxes are considered in the context of passing through the resonator from the moment of exceeding the threshold for laser action. The radiation which is generated in an active multicore fibre does not propagate through the cores only, but to some extent it penetrates into the cladding. Accordingly, the size of the mode is greater than the core diameter, depending on the normalized frequency of the fibre. If the arrangement of cores enables partial exchange of radiation between them, then, as a result, apart from amplitudes, also the phases of the generated radiation are modified.

For the purpose of analysis, it was assumed that the fibre of length L consists of n fundamental segments of length $\Delta z = 1$ cm. In each of these segments, the amount of exchanged energy equals $\Delta C = C/n$ (where C – total exchanged radiation energy over the length L of the fibre). Furthermore, for each segment Δz the gain factor of active medium has to be taken into account; its value changes in the function of fibre length. Figure 8 illustrates the concept of phase locking of radiation generated in individual cores which occurs through partial exchange of the radiation in effect of coupling between cores. To explain the mechanism of this phenomenon the example of an active fibre with two cores working as a fibre laser is used. During each pass of the photon flux through the resonator, partial exchange of the generated radiation between the neighbouring cores takes effect. In this way, the phase difference between radiation in the cores decreases after every pass.

The expression $C \cdot J_i$ determines the energy transferred as a result of coupling between the cores. The radiation in each core can be expressed in the form of a vector: $J_i = A_i \exp(i\varphi_i)$ where A_i is the field amplitude, and φ_i the phase.

$$J_n^{\pm ai}(z) = A_n^{\pm ai} e^{j\varphi_n^{\pm ai}}. \quad (7)$$

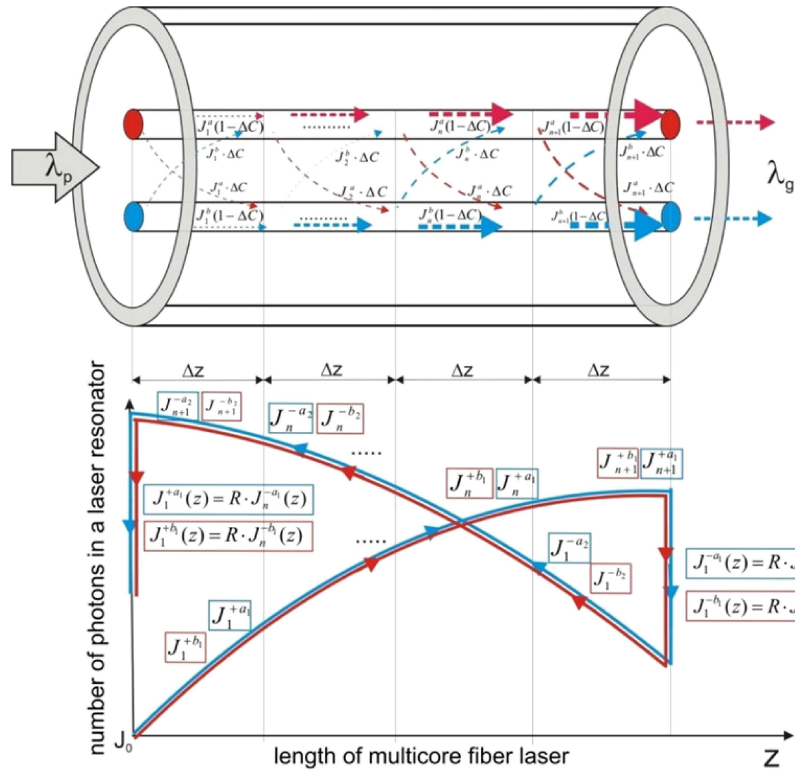


Fig. 8. The idea of phase-locking of the radiation as a result of coupling between the cores exemplified by a double-core active optical fibre operating in a fibre laser system:

- $J_1^{+a_i}$ – the vector describing the generated radiation propagating in Core 1 before the first passage of the photon flux through a resonator,
- $J_1^{+b_i}$ – the vector describing the generated radiation propagating in Core 2 before the first passage of the photon flux through a resonator,
- $J_n^{+a_i}$ – the vector describing the generated radiation propagating in the a -th core after the n -th (i – calculation step) passage of the photon flux through a resonator,
- $J_n^{+b_i}$ – the vector describing the generated radiation propagating in the b -th core after the n -th (i – calculation step) passage of the photon flux through a resonator,
- $\varphi_n^{+a_i}$ – the phase of the radiation propagating in the a -th core after the n -th (i – calculation step) passage of the photon flux through a resonator,
- $\varphi_n^{+b_i}$ – the phase of the radiation propagating in the b -th core after the n -th (i – calculation step) passage of the photon flux through a resonator,
- $\Delta\varphi^n$ – the phase difference of the generated radiation after the n -th passage of the photon flux through a resonator

Calculations were carried out for all the analyzed designs of multicore fibres, assuming the following parameters:

- $L = 5$ m – the fibre length,
- $2r = 10 \mu\text{m}$ – diameter of the cores,
- the initial phase of the radiation generated in the cores is random,
- $\sigma_e = 1 \cdot 10^{-20} [\text{cm}^2]$ – emission cross-section,
- $\alpha_a = 46 \text{ cm}^{-1}$ – absorption coefficient of pump radiation,
- $\alpha_p = 0.4 \text{ cm}^{-1}$ – optical losses without taking into account the absorption coefficient,
- $\alpha = 0.46 \text{ cm}^{-1}$ – absorption coefficient of the cores,
- A_r – cross-sectional area of the cores,
- $N_0 = 2 \cdot 10^{19} [\text{ions/cm}^3]$ – concentration of rare – earth (Yb^{3+}),
- $\beta_1 = \beta_2 = \beta_n$ – propagation constant of cores,
- $\tau = 2$ [ms] – lifetime at the upper laser level,
- $C = (1 - 10)\%$ – coupling coefficient between the cores along the whole fibre length optical fibre with zero attenuation,
- $P_{\text{pump}} = 10$ W.

Optical gain in the discussed structure is described by the relations:

core a

$$k_{i+1}^{+a}(z_n) = \frac{\sigma_e \tau}{h\nu_p A_r} \alpha_a P_P(0) \exp[-(\alpha_a + \alpha_p) n \cdot \Delta z] \cdot \frac{1}{1 + (P_i^{+a}(z) + P_i^{-a}(z))/P_s} \quad (8)$$

$$k_{i+1}^{-a}(z_n) = \frac{\sigma_e \tau}{h\nu_p A_r} \alpha_a P_P(0) \exp[-(\alpha_a + \alpha_p) (z - n \cdot \Delta z)] \cdot \frac{1}{1 + (P_i^{+a}(z) + P_i^{-a}(z))/P_s} \quad (9)$$

core b

$$k_{i+1}^{+b}(z_n) = \frac{\sigma_e \tau}{h\nu_p A_r} \alpha_a P_P(0) \exp[-(\alpha_a + \alpha_p) n \cdot \Delta z] \cdot \frac{1}{1 + (P_i^{+b}(z) + P_i^{-b}(z))/P_s} \quad (10)$$

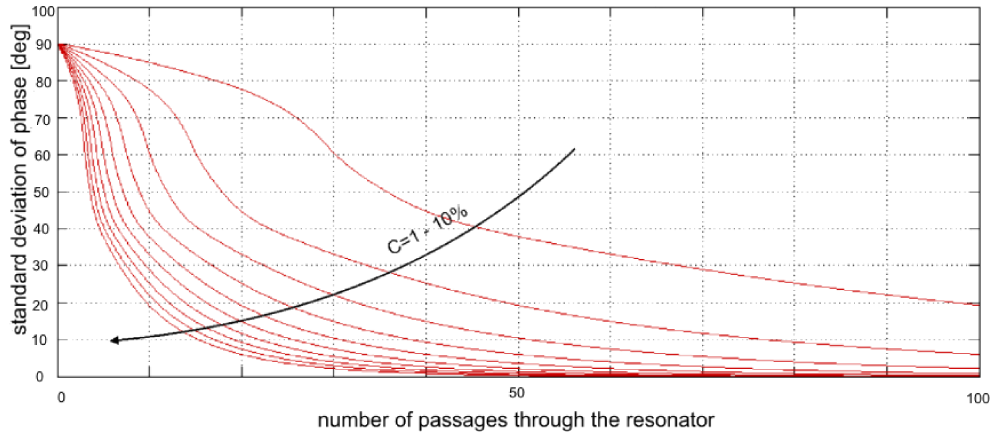


Fig. 9. Standard deviation of phase of the radiation generated in all cores in the function of the number flux passes through the resonator (19-core fibre)

$$k_{i+1}^{-b}(z_n) = \frac{\sigma_e \tau}{h\nu_p A_r} \alpha_a P_P(0) \exp[-(\alpha_a + \alpha_p)(z - n \cdot \Delta z)] \cdot \frac{1}{1 + (P_i^{+b}(z) + P_i^{-b}(z))/P_s}, \quad (11)$$

where $P_p(0)$ – pump power at the entrance to the fibre, α_a – the effective absorption coefficient at the pump wavelength, α_p – loss coefficient of the fibre at the pump wavelength accounting for all loss mechanisms, σ_e – emission cross section, A_r – cross-section area of the fibre core, $h\nu_p$ – pump photon energy, P_s – saturation output power, $k_{i+1}^{+a}(z_n)$ – gain in core **a**, in the n -th iteration during the $i + 1$ -th pass of the photon flux through the resonator in the “+” direction, $k_{i+1}^{-a}(z_n)$ – gain in core **a**, in the n -th iteration during the $i + 1$ -th pass of the photon flux through the resonator in the “–” direction, $k_{i+1}^{+b}(z_n)$ – gain in core **b**, in the n -th iteration during the $i + 1$ -th pass of the photon flux through the resonator in the “+” direction, $k_{i+1}^{-b}(z_n)$ – gain in core **b**, in the n -th iteration during the $i + 1$ -th pass of the photon flux through the resonator in the “–” direction.

Boundary conditions arising from the reflection of the photon flux from the ends of the active fibre are:

$$J_1^{-a_i}(z) = R \cdot J_n^{+a_i}(z), \quad (12)$$

$$J_1^{-b_i}(z) = R \cdot J_n^{+b_i}(z), \quad (13)$$

$$J_1^{+a_1}(z) = R \cdot J_n^{-a_1}(z), \quad (14)$$

$$J_1^{+b_1}(0) = R \cdot J_n^{-b_1}(0). \quad (15)$$

Boundary conditions: $P_0 = h\nu_s (\pi\Delta\nu_s/2)$ – initial power associated with a single pass of photons in the band $\Delta\nu$, where $h\nu_s$ – energy of photons of the generated radiation.

Total output flux can be described as:

$$J_{wy}^{a_i} = (1 - R)J^{+a_i}(z), \quad (16)$$

$$J_{wy}^{b_i} = (1 - R)J^{+b_i}(z). \quad (17)$$

The calculated phase locking degree of the radiation generated in the cores of a multicore fibre, described by standard deviation of phase in the function of the number flux passes through the resonator, for the coupling value $C = (1 - 10)\%$ is shown in Fig. 9.

In the investigated fibre, exchange of minimum 5% of the generated radiation between the cores at the fibre length $L = 5$ m caused radiation phase locking in all the 19 cores after less than 100 passes of the flux through the resonator in linear multicore fibre laser system. Then, in the Fraunhofer diffraction region a central peak of high intensity (supermode) could be observed, together with symmetrically located side lobes.

4. Experiments

In order to establish the composition with the optimal luminescent properties, several batches of aluminosilicate glass were produced as matrices for rare earth elements. The composition of the glasses was following: (40–60)SiO₂ – (6–10)Al₂O₃ – (6–8) PbO – (6–8)B₂O₃ – (2–4) BaO – (8–12)Na₂O – (6–8)K₂O – (0.15–0.5)Yb₂O₃ mol%. Glasses were synthesized by conventional melting and quenching method in covered platinum crucibles, in an electric furnace, at temperature of 1400–1450°C and annealed at temperature range 400–450°C. As a result, transparent and homogeneous glass rods were obtained, which were subsequently used for creation of cores and cladding of a double-clad 19-core active fibres. The absorption cross-section of thus produced ytterbium-doped glass was determined with the aid of spectral transmission measurement results. As for the emission cross-section, it was calculated relying on the Fuchtbauer-Ladenburg formula. Thermal properties of the glass were analyzed using a Setaram Labsys scanning differential calorimeter. Then, the glass was pulverized, and the samples of about 35mg were heated up from room temperature to 1000°C in a platinum crucible with a rate of 10°C/min in nitrogen atmosphere. Coefficient of thermal expansion was denoted for samples with dimensions of 3×5×20 [mm] heated up from room temperature to 600°C with a rate of 10°C/min. The obtained curve allowed

for establishing transition (T_g) and softening (T_m) temperatures. Refraction index for the wavelength of 633 nm was measured with the use of a Metricon 2010/M Prism Coupler refractometer. For each batch, glass density was measured by hydrostatic weighing. All the conducted simulations were necessary to discover the material and geometrical parameters of the active 19-core fibre which would meet the requirements of internal phase-locking of the generated radiation. The fibre itself was created with a specially modified for the purpose rod-in-tube technique. Luminescence measurement unit included: thermally stabilized HLU25F200-980 laser diode with a fibre-coupled output, a system for formation and injection of laser beam, Acton Spectra Pro 2300i monochromator, and a Stellarnet Blue Wave spectrometer.

Figure 10 presents cross-section of the fabricated 19-core optical fibre doped with 0.15mol%. The produced 19-core fibre was marked by high luminescence. High numerical aperture of the inner cladding facilitated effective pumping. The fibre was excited by a semiconductor laser diode emitting radiation of 976 nm wavelength.

Typically for ytterbium, emission band at about 1030 nm was presented in Fig. 11. Radiation emission wavelength of about 980 nm corresponding to the three-level scheme and probably overlapping with optical pumping radiation. Observation of the far-field pattern generated by the 19-core fibre was carried out in a configuration MOFPA in which the seed laser was formed by a fibre laser based on the ytterbium-doped NUFERN LMA 20/400 fibre (FWHM=1 nm). The seed laser was being excited by a laser diode emitting radiation of 976 nm wavelength ($P_{\max} = 25$ W). The investigated 19-core Yb^{3+} -doped fibre with a hexagonal core arrangement was pumped by a laser diode emitting radiation of 940 nm wavelength ($P_{\max} = 25$ W) through the side fibre coupler. The experimental setup was presented in Fig. 12. The far-field pattern was recorded in the distance of 1 cm from the fibre output, with a Newport KEP-3-IR3 laser beam profile analyzer is shown in Fig. 13.

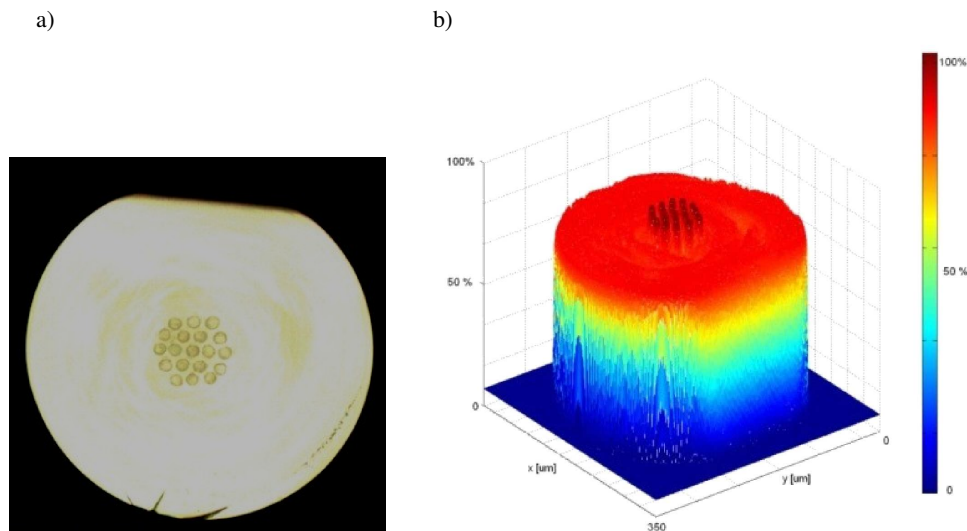


Fig. 10. Cross-section (a) luminance distribution (b) of the fabricated 19-core optical fibre doped with 0.15mol% Yb_2O_3

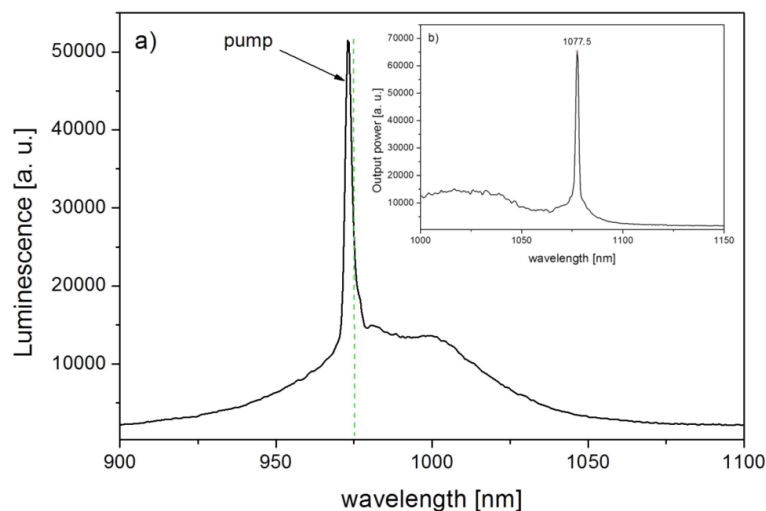


Fig. 11. Luminescence spectra of the fabricated optical fibre doped with Yb^{3+} ($\lambda_p = 980$ nm) (a), Output spectra of the SEED NUFERN fibre laser doped with Yb^{3+} (b)

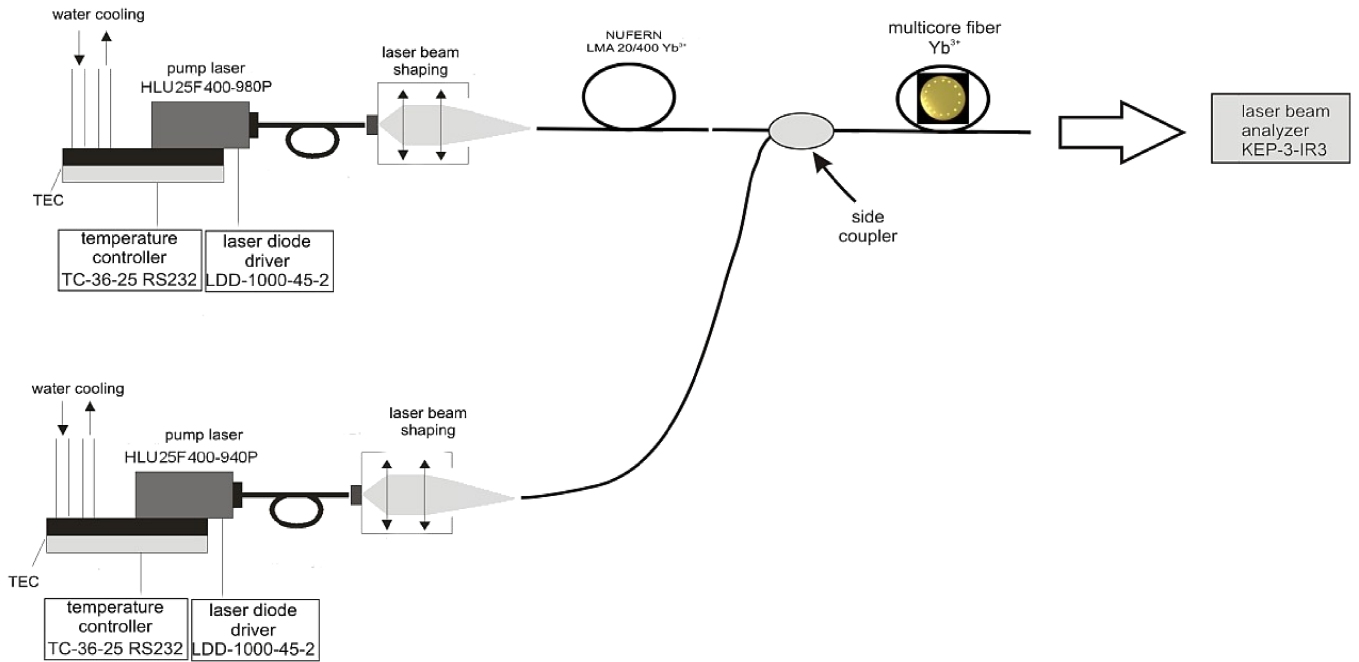


Fig. 12. Experimental setup

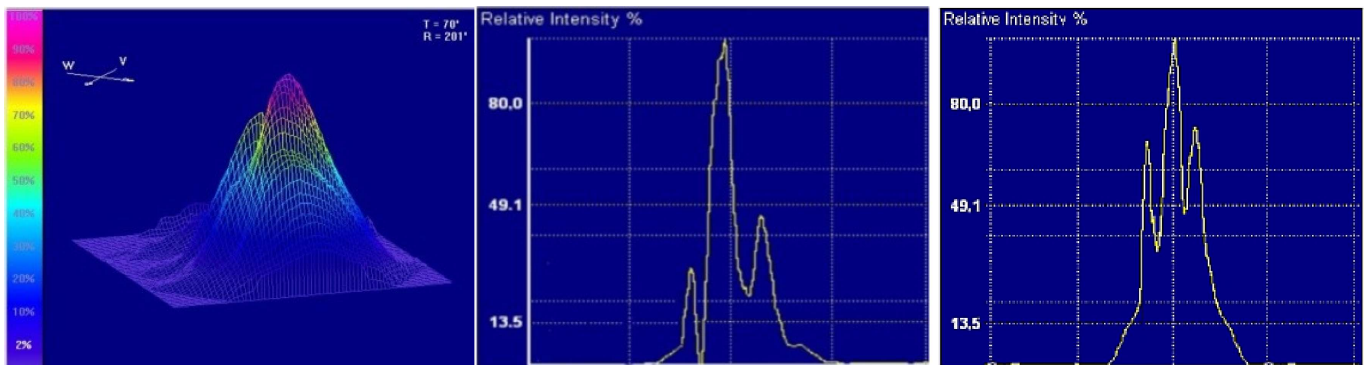


Fig. 13. Far-field pattern registered in 19-core Yb^{3+} -doped fibre

The far-field pattern registered in the course of the experiment turned out to have a similar shape to the one which had been numerically calculated with the assumption of phase coherence between the radiation propagated in the cores. It consisted of a centrally-located peak and symmetrically located side-lobes, which confirms the effect of internal phase-locking of radiation in the discussed fibre.

Table 1

Basic physicochemical properties of aluminosilicate glasses

Property	Value
Density [g/cm^3]	3.08–4.21
Index of refraction $\lambda = 633 \text{ nm}$	1.62–1.64
Concentration of Yb_2O_3 [ion/cm^3]	$2\text{e}+19$
$\sigma_{abs}(\text{Yb}^{3+})$ [cm^2]	$3\text{e}-21$
$\sigma_{em}(\text{Yb}^{3+})$ [cm^2]	$3.3\text{e}-21$
Thermal expansion coefficient. α (100–400°C) [10^{-7}K^{-1}]	75–85
Transition temperature T_g [°C]	435–480°C

Table 2

Properties of the fabricated optical fibre

Property	Value
Outer diameter [μm]	350
Diameter of cores [μm]	11
NA_{cores}	0.07
$\text{NA}_{cladding}$	0.58

5. Conclusions

Double-clad multicore active optic fibres whose cores generate mutually coherent radiation open new possibilities for construction of high-power fibre lasers. The conducted numerical analysis of structural parameters unambiguously confirmed that the optimum $\text{BQF} = 0.91$ is achieved when the structural parameters of active multicore fibre are as follows: $d = 18 \mu\text{m}$, $V = 1.7$. Moreover, standard deviation values less than 14° remain without any significant influence on the far-field patterns in the tested fibres. Relative decrease of

BQF in this range is lower than 0.3%. Analysis of required conditions and practicability of generating a supermode in the 19-core active fibre with a hexagonal core arrangement working as a fibre laser presented in the article proved that in the said fibre laser, the exchange of minimum 5% of the radiation generated between the neighbouring cores over the entire length of the fibre ($L = 5$ m) causes phase-locking of the radiation after less than 100 passes of the photon flux through the resonator, counting from the moment of exceeding the laser action threshold in linear fibre laser. The produced ytterbium-doped 19-core fibre was characterized by structural parameters meeting the numerically-determined conditions for phase-locking of the radiation generated in the cores. As well as that, the fibre was marked by high luminescence in the band of about 1030 nm. Registered in the course of the experiment in MOFPA system far-field pattern showed centrally located peak of relatively high radiation intensity together with smaller side-lobes, and as such was similar to the pattern which had been obtained numerically. This means that it is viable to apply the designed fibres as active media for construction of lasers which employ the coupling of radiation between cores into the single supermode.

Acknowledgements. This work was supported by the Ministry of Science and Higher Education of Poland – grant No. N N507 285636 and the work of Białystok University of Technology No. S/WE/2/08.

REFERENCES

- [1] N.N. Elkin, A.P. Napartovich, V.N. Troshchieva, and D.V. Vysotsky, “Diffraction modeling of the multicore fibre amplifier”, *J. Lightwave Technology* 25 (10), 3072–3077 (2007).
- [2] X. Zhu, A. Schülzgen, X. Li, H. Li, V.L. Temyanko, J.V. Moloney, and N. Peyghambarian, “Birefringent in-phase supermode operation of a multicore microstructured fibre laser”, *Optics Express* 15 (16), 10340–10345 (2007).
- [3] P.R. Kaczmarek, G. Soboń, J.Z. Sotor, A.J. Antończak, and K.M. Abramski, “Fiber-MOPA sources of coherent radiation”, *Bull. Pol. Ac.: Tech.* 58 (4), 486–489 (2010).
- [4] D. Dorosz, M. Kochanowicz, “Model analysis of supermode generation in active 5-core optical fibre”, *Opto-Electron. Rev.* 18 (4), 40–45 (2010).
- [5] T. Pustelny, C. Tyszkiewicz, and K. Barczak, “Optical finer sensors of magnetic field applying Faraday’s effect”, *Optica Applicata* 32 (2–3), 469–475 (2003).
- [6] Y. Kono, M. Takeoka, K. Uto, A. Uchida, and F. Kannari, “A coherent all-solid-state laser array using the talbot effect in a three-mirror cavity”, *IEEE J. Quantum Electronics* 36 (5), 607–614 (2000).
- [7] A. Desfarges-Berthelelot, V. Kermene, D. Sabourdy, J. Boullet, R. Philippe, J. Lhermite, and A. Barthélémy, “Coherent combining of fibre lasers”, *C. R. Physique* 1, 244–253 (2006).
- [8] D. Dorosz, “Rare earth ions doped aluminosilicate and phosphate double clad optical fibres”, *Bull. Pol. Ac.: Tech.* 56 (2), 103–111 (2008).
- [9] A. Zajac, D. Dorosz, M. Kochanowicz, M. Skórczakowski, and J. Świdorski, “Fibre lasers – conditioning constructional and technological”, *Bull. Pol. Ac.: Tech.* 58 (4), 491–502 (2010).
- [10] D. Dorosz and M. Kochanowicz, “Multicore optical fibre doped with neodymium”, *Proc. SPIE* 7120, 71200H-1-71200H-5 (2009).
- [11] A.P. Napartovich and D.V. Vysotsky, “Phase – locking of multicore fibre laser due to Talbot self – reproduction”, *J. Modern Optics* 50 (18), 2715–2725 (2003).
- [12] M. Wrage, P. Glas, M. Leitner, D.V. Vysotsky, and A.P. Napartovich, “Phase – locking and self – imaging properties of a Talbot resonator applied to circular structures”, *Optics Communications* 191, 149–159 (2001).
- [13] Y. Li, L. Qian, D. Lu, D. Fan, and S. Wen, “Coherent and incoherent combining of fiber array with hexagonal ring distribution”, *Optics & Laser Technology* 39, 957–963 (2007).
- [14] D. Dorosz, J. Swiderski, and A. Zajac, “Double clad aluminosilicate optical fibre doped with Nd^{3+} ions”, *Eur. Phys. J. Special Topics* 154, 51–56 (2008).
- [15] Z. Chen, J. Hou, P. Zhou, X. Wang, X. Xu, Z. Jiang, and Z. Liu, “Mutual injection locking and coherent combining of three individual fibre lasers”, *Optics Communications* 282, 60–63 (2009).
- [16] Y. Ma, P. Zhou, X. Wang, K. Han, H. Ma, X. Xu, L. Si, Z. Liu, and Y. Zhao, “Coherent beam combination of two thulium-doped fiber laser beams with the multi-dithering technique”, *Optics & Laser Technology* 43, 721–724 (2011).
- [17] Z. Chen, J. Hou, P. Zhou, and Z. Jiang, “Mutual injection-locking and coherent combining of two individual fibre lasers”, *IEEE J. Quantum Electronics* 44 (6), 1168–1175 (2008).
- [18] M. Kochanowicz, D. Dorosz, and J. Żmojda, “Phase-locking of 7-core Yb^{3+} -doped optical fibre”, *Proc. SPIE* 7745, 77450M-1-77450M-10 (2010).
- [19] M. Kochanowicz, D. Dorosz, J. Dorosz, and J. Żmojda, “Phase-locking of optical fibre with hexagonal cores array doped with neodymium”, *Proc. SPIE* 7721, 772110-1-772110-9 (2010).
- [20] P. Zhou, Z. Liu, X. Xu, Z. Chen, and X. Wang, “Beam quality factor for coherently combined fibre laser beams”, *Optics & Laser Technology* 4, 1268–271 (2009).
- [21] M. Kochanowicz, D. Dorosz, J. Żmojda, and J. Dorosz, “Beam quality of multicore fibre lasers”, *Acta Physica Polonica A* 118, 1177–1182 (2010).
- [22] J. Petykiewicz, *Wave Optics*, Publishing House of Warsaw University of Technology, Warsaw, 1986, (in Polish).
- [23] S.M. Schultz, “Using MATLAB to help teach Fourier optics”, *Proc. SPIE* 6695, 66950I-1-66950I-10 (2007).